1 **Title:** Character integration, preadaptation, and the evolution of evolvability in apes

2 **Author:** Caroline Parins-Fukuchi*[1,2]

3 [1]Department of Geophysical Sciences, University of Chicago, Chicago, IL, USA

4 [2]Department of Ecology and Evolutionary Biology, University of Michigan, Ann Arbor,

5 MI, USA

6 *Author for correspondence: parinsfukuchi@uchicago.edu

7 **Data archived online:** https://figshare.com/articles/parins-fukuchi_supp_zip/8063726

8

9 **Funding**

10 A portion of this work was carried out while the author was supported by a Predoctoral

11 Fellowship provided by the Rackham Graduate School at the University of Michigan.

12

13 **Acknowledgements**

14 I wish to thank D Alvarado-Serrano, M Cosman, CW Dick, DC Fisher, LM MacLatchy,

15 H Marx, J Saulsbury, SA Smith, N Walker-Hale for conversations that have greatly

16 benefitted this work. I also thank S Worthington for help accessing his skeletal

17 measurements that comprised a large portion of the character matrix analyzed here. I also

18 think P Wagner and one anonymous reviewer for comments that substantially improved

19 the manuscript.

20

21

22

**Abstract:** A central research program in evolutionary biology over the past 50 years has involved interpreting macroevolutionary patterns, such as key innovation and preadaptation, as mediated by interactions between single phenotypic traits and shifting ecological landscapes. While this focus has generated substantial evidence for the potency of environmental pressures in driving evolutionary changes, it has also created conceptual frustrations. I present analyses of a character matrix sampled across the haplorrhine skeleton that revealed several suites of integrated characters displaying distinct patterns in macroevolutionary disparity throughout the Miocene. Comparison of these patterns to those in neurological development revealed general support for a pattern in evolutionary and developmental flexibility shared by all great apes. Shifting and reduced constraint in apes was met with episodic bursts in phenotypic innovation that built a wide array of functional diversity over a foundation of shared developmental and anatomical structure that was laid throughout the Miocene. Notably, both apes' exceptional morphological disparity and humans' phenotypic distinctiveness can both be explained by earlier shifts in integration. These patterns demonstrate that relaxation of integration can correspond to enhanced evolvability that has a 'preadaptive' effect by catalyzing later episodes of dramatic morphological remodeling.

Keywords: integration, evolvability, preadaptation, diversification, hominoidea

## Introduction

Developing a better understanding of the adaptive drivers of evolutionary change has long been a central goal in paleontology and comparative biology. When inquiring at macroevolutionary timescales, it is generally not possible to reconstruct natural selection regimes operating at the population level. However, researchers have long analyzed patterns in phenotypic evolution within the context of ecological and environmental shifts to better understand the adaptive landscape underlying major shifts in body plan and the emergence of novel biological functions (Simpson 1944). For example, many comparative studies seek to identify correlations between macroevolutionary diversification (encompassing both phenotypic disparity and speciation) and the emergence and colonization of new ecological niches. Many of these studies have found that shifts in the evolutionary rate of phenotypic characters, such as body size, coincide with those in ecological traits, such as climatic variables and biogeography (Harmon et al., 2003, Losos et al., 2006, Mahler et al., 2013, Slater and Friscia 2018). There is also evidence in some taxa that elevated rates of phenotypic evolution may sometimes correspond to elevated rates of lineage diversification (Rabosky et al. 2013; but see Crouch and Ricklefs 2019).

The early focus on environmental adaptation was first codified through the conceptual application of modern synthesis-era population genetic theory to questions at the macroevolutionary scale. George Gaylord Simpson combined quantitative descriptions of selection, drift, and fitness landscapes developed during the synthesis to suggest that large evolutionary changes occur rapidly as species move between and

optimize their position within 'adaptive zones' shaped by ecology. In this illustration, each zone is represented as an adaptive peak on a multi-dimensional fitness landscape, each of which describes a locally optimal combination of phenotypes. Although initially maintaining position on a single peak due to stabilizing selection, Simpson hypothesized that genetic drift may cause species to descend and cross adaptive valleys, during which positive selection re-emerges to propel the species to a new peak. This image has been influential, providing the theoretical basis for major evolutionary concepts. For example, large evolutionary radiations are often hypothesized be limited in their intensity by the availability of new ecological opportunities through environmental changes or improvement of competitive ability (Rainey and Travisano 1998, Yoder et al., 2010, Wagner and Harmon et al 2012, but see Slater 2015).

The role of ecological processes in generating morphological novelty can be contrasted with an increasing focus on 'constructional' factors that include functional interactions and architectural constraints (Seilacher 1970, 1991). While character evolution may sometimes reflect simple optimization processes when natural selection operates independently on separate traits, the evolutionary pathways realized in nature are also constrained by the complex interactions between functionally dependent traits and the limitations of an organism's developmental architecture. When placed into a broader evolutionary literature, these limiting factors might be coarsely partitioned into developmental (Gould and Lewontin 1979, Olson 2012) and functional (Charlesworth et al., 1982, Cheverud 1984, Maynard-Smith et al., 1985) constraints.

One characterization of developmental constraint involves the tight linkage of characters in ontogeny through factors that include allometry and modularity. When traits are developmentally linked, but functionally autonomous, the available set of selectively advantageous modifications belonging to one is limited by the fitness effect on the other. Wagner and colleagues (2007) formulated an example of such patterns using vertebrate limbs. While fore- and hindlimbs are functionally independent in many species, their shared origin as serial homologs causes quantitative variation in each set of limbs to be correlated through their linkage in development. Developmental constraints are also frequently characterized by the set of fundamental limitations imposed on an organism's form by its developmental programming. This article will focus most heavily on the former aspect of developmental constraint.

Functional constraint exists when multiple traits contribute to a shared function that is under selection and/or when a single trait performs multiple functions that are each under selection. Although any particular trait may perform many functions that contribute to fitness in different ways, the phenotype for each trait that contributes to a shared function that is under strong selection will be limited to values that facilitate its contribution alongside the other constituent traits.

Shared developmental pathways and multivariate selection, along with related processes such as epistasis and pleiotropy, can act and interact in complex ways to yield similar patterns. Although it is usually impossible to distinguish between each of these processes in historical, macroevolutionary study systems, they share a common tendency to drive the formation of modules of characters that are linked in their evolutionary

110 trajectories through a higher-level process traditionally referred to as 'integration' (Olson
111 and Miller 1958). An understanding of integrated and modular evolution has facilitated
112 study of the ways that Simpson's classic conception of ecological adaptation at
113 macroevolutionary scales is mediated by the multivariate complexity of reality. While
114 ecological pressures undoubtedly shape evolutionary trajectories, developing a holistic
115 understanding of the ways that development and the functional interdependence of
116 characters constrain evolvability will enhance our knowledge of the macroevolutionary
117 processes that drive the emergence of phenotypic novelty throughout deep time.

118 Developmental and functional constraints influence evolution in significant ways.
119 For example, when ecological opportunity is abundant, evolutionary radiations can be
120 driven primarily by the release of developmental constraints (Wagner et al. 2003). This
121 conception runs the risk of false dichotomy between ecology and constraint in the sense
122 that relaxed constraint may itself be driven by ecological factors, but this simplification
123 does not negate the insight that both constraint and ecological opportunity can be limiting
124 factors in clade disparification. Reductions in developmental constraint can also shape
125 macroevolutionary patterns by driving increases in evolutionary rate (Donoghue and Ree
126 2000). This pattern appears to hold for integration more generally, with higher degrees of
127 integration often linked to lower evolutionary disparity and rate (Goswami et al. 2014,
128 2015). Integration, as reflecting developmental and/or functional interactions between
129 traits, may constrain the possible range of phenotypes that a character might display
130 because of the fitness consequences of its modification upon other characters that are
131 linked either by development or shared function.

Understanding the set of evolutionary limitations imposed by integration through development and functional constraints is crucial in determining the capacity for a clade to diversify phenotypically. Together, these factors might be said to determine the level of 'constructional opportunity' available at a given time. Considered in opposition to ecological opportunity (Losos 2010), constructional opportunity reflects the evolvability of a clade that is determined by the level of constraint imposed by the structure of developmental and functional interactions between characters, as well as other architectural considerations (Turing 1953, Raup 1966). While ecological opportunity is often evoked as a limiting factor on a clade's phenotypic diversification, constructional opportunity may also limit the range of evolutionary modifications available to a population faced with ecological pressure.

Apes have been extensively studied in the context of both developmental constraint and environmental adaptation. Young et al. (2010), found that apes display weak integration between the fore- and hindlimb in comparison to cercopithecoids. Reduced integration can confer greater functional flexibility, and so may have facilitated the proliferation of the diverse locomotor function across living and fossil apes. Changes in developmental timing have also been important in ape evolution. Developmental heterochrony appears to have driven the emergence of many key aspects of hominin morphology in the cranium and post-cranium (Gould 1977, Berge 1998). This long-standing interest in the developmental basis of ape evolution has not excluded environmental hypotheses. Environmental fluctuations throughout the Miocene and Pliocene have also frequently formed the basis for adaptive hypotheses across apes

(Andrews 1992, Ruff 1994, Michel et al., 2014). The body plans of hominins, and undoubtedly apes in general, have been shaped through modifications to separate suites of traits occurring at different times (Holloway 1973, McHenry 1975). These diverse threads suggest that a multiplicity of causes, perhaps including both ecological opportunity and constructional factors, has shaped the evolution of hominoid body plans. As a result, apes are an excellent exemplar taxon in which to pluralistically examine the mosaic patterns in constraint and innovation that shape body plans in living and fossil vertebrates.

In this study, I sought to examine whether the relaxed integration shared by great apes corresponds to elevated rates of evolutionary disparification in morphological and developmental traits across all apes. To address these questions, I reconstructed the mosaic macroevolutionary patterns in morphological, neurological, and developmental phenotypes across living and fossil great apes throughout the Miocene. To help place these empirical results in a theoretical context, I also present a set of simple simulations to generate a theoretical expectation for the patterns in disparity expected when Markovian diffusion is constrained by both selection and development. Taken together, these analyses suggest the capability for shifting patterns in constraint to create constructional opportunities that generate repeated and dramatic episodes in morphological innovation.

## Methods

### *Morphological data*

I gathered a dataset of 149 quantitative morphological traits from the literature (Lewton 2010, Worthington 2012) spanning the cranium, forelimb, and pelvis. These traits were sampled across 10 extant taxa. I also collected fossil cranial and forelimb traits from Worthington (2012), retaining all taxa with at least 25% matrix occupancy. Taxa were all studied at the generic level, with each extant genus represented by a single exemplar species. Each morphological trait represented a dimensionless ratio or geometric mean. I scaled the traits to display an empirical variance of 1 across all taxa. This simplified the analyses by reducing the complexity of the dataset, while retaining the same comparative information. Since the original traits were dimensionless, both the unscaled and the scaled datasets would facilitate examination of *relative*, rather than absolute, evolutionary rates, but the scaled traits improve Markov-chain Monte Carlo (MCMC) mixing and simplify the identification of mosaic suites.

*Neurological data*

To directly study the evolutionary patterns in related developmental and phenotypic traits, I also gathered neurological data from the literature (Capellini et al., 2010, Boddy et al., 2012). For neurological phenotype, I collected encephalization quotients (EQ) estimated in 76 primate species by Boddy et al. (2012). EQ is calculated by fitting a nonlinear model to brain size and body size and taking the deviations (residuals) from the best fit curve and so measures the enlargement of brain size while controlling for allometry with body size. I compared EQ patterns to those in a postpartum encephalization development (ED) metric calculated as:

$$ED = EQ_{adult} - EQ_{neonatal} \quad (1)$$

ED is therefore intended to reflect the amount of brain tissue grown by members of each species following birth relative to their body size. Neonatal brain and body mass data representing 24 primate species were acquired from Capellini et al. (2010).

*Fossil placement and divergence time estimation*

Since the evolutionary relationships between the extant taxa represented in the morphological dataset have all been extensively studied and are well-resolved, I used these as a fixed scaffolding to place the fossil taxa. Fossil placements were inferred from the continuous trait dataset using the cophymaru program (Parins-Fukuchi 2018). I used the 'binary weights' procedure to filter out reliable traits from ones likely to mislead by using the extant tree as a fixed point of reference. Markov-chain Monte Carlo (MCMC) simulations were run for 1,000,000 generations and checked manually for convergence. The posterior tree sample was summarized as the maximum clade credibility tree using sumtrees.py (Sukumaran and Holder 2010).

For downstream comparative analyses, I also estimated divergence times on the full 19-taxon tree. I downloaded cytochrome B sequences from Genbank representing each of the 10 extant taxa. Molecular dating was performed using Beast version 2.4.8 (Bouckaert et al. 2014) using the fossilized birth-death (FBD) prior. The topology was fixed to the summary tree generated during the fossil placement step. Temporal occurrence ranges for the fossil taxa were assembled from the literature. These fossil and extant occurrence ranges were used in the dating analysis to infer the diversification and sampling rate parameters used in the FBD prior.

*Measuring evolutionary integration*

As a preliminary evaluation of the strength of integration in the skeletal traits across the haplorrhine phylogeny, I calculated the phylogenetic independent contrasts (PIC) (Felsenstein 1985) at each node in a tree of nine extant haplorrhine taxa (*Pan paniscus* was removed because it was missing pelvic measurements). At each internal node in the phylogeny, I then calculated the correlation between the vector of characters at each child node. Stronger correlations are expected to correspond to tighter integration. If the child represented an internal node, the PIC values were used as the character vector. PICs were calculated on the dated phylogeny, with the fossil taxa pruned.

*Evolutionary rates across mosaic morphological suites*

I used the *greedo* program to recover mosaic patterns in disparity from the continuous trait dataset (Parins-Fukuchi 2019). *Greedo* is a phylogenetic clustering/mixture model estimation approach that uses the Akaike information criterion (AIC) to iteratively merge and split clusters of traits to find a best-supported set of character suites based on shared patterns in disparity, where each is represented by a tree with branch lengths (Fig. 1). Traits that display the highest improvement in log-likelihood when assigned to a separate cluster are prioritized during the splitting steps to first identify likely sources of heterogeneity in the dataset. During the merging step, only clusters that show an improved AIC score when placed under the same model are joined. This process recovers an estimate of the number of suites, the membership of each trait, and a tree with branch lengths scaled to units of disparity for each suite. Fossil taxa were not included in the mosaic analyses, because they were too fragmentary in their sampling to inform disparity patterns when the traits were split into suites. I performed many runs

241 of the *greedo* procedure to avoid presenting results obtained from a suboptimal peak on
242 the likelihood surface. Since several of the top clusterings yielded close AIC support, I
243 performed an additional model-averaging step using Akaike weights to summarize the
244 results as a graph where each trait occupies a node, and each link is weighted to reflect
245 the total weighted AIC support across all the models. Comparative analyses were
246 performed using a single summary clustering that resulted from application of the
247 Markov clustering (MCL) algorithm to the support network (Dongen 2000).
248 To examine the anatomical composition of the mosaic suites of characters, I
249 performed a statistical enrichment procedure to identify skeletal regions that were over
250 and under-represented in each suite relative to the proportions for each present in the
251 entire dataset. The proportion of the 149-trait dataset represented by each skeletal region
252 was used to generate a set of 'expected' values. I then compared these to the observed
253 proportions within each suite to examine trends in the deviations of the proportions
254 occupied by each region. I did not assess the statistical significance of these deviations,
255 because 1) my aim was to examine the general patterns in the composition of each
256 character suite rather than to determine absolute significance, and 2) the small sample
257 size of the dataset generated expected chi-square test statistic values that were nearly
258 entirely <5, making the test inappropriate. To examine the relative contributions of
259 separate anatomical regions in shaping the macroevolutionary patterns reconstructed in
260 each suite, I also performed a principal component analysis (PCA) on the traits contained
261 within each suite. I then transformed the loadings to calculate the total variance

262 contributed by each trait across all axes of the PCA, summing them to produce the
263 contribution of each anatomical region.

264 I transformed the branch lengths for each mosaic suite, which were scaled to
265 reflect disparity (total variance, *v*, accumulated over time *t*), to rates (*v* per unit *t*) using
266 the results from the divergence time analysis. I also calculated evolutionary rates
267 averaged over the entire morphological dataset while including the fossil taxa to coarsely
268 reconstruct evolutionary tempo throughout the Miocene. Although this step missed
269 valuable information recovered by the mosaic analyses, including the fossil taxa in this
270 manner enabled finer resolution into the coarse patterns in evolutionary tempo throughout
271 the Miocene.

272 *Evolutionary rates in neurological data*

273 I estimated macroevolutionary rates across primates in ED and EQ using BAMM
274 version 2.5.0 (Rabosky 2014). Since the trees that I constructed for the morphological
275 analysis contained only a fraction of the taxa present in the neurological datasets, I used
276 the dated primate supertree packaged in BAMM that was originally sourced from Mos
277 and Mooers (2006) and pruned the tips to match the taxa present in each dataset. MCMC
278 simulations were run until the estimated sample size (ESS) well exceeded 200 for each
279 parameter. Results were presented by plotting the mean rate estimated along each branch
280 and the maximum *a posteriori* configuration of rate shifts using BAMMtools version
281 2.5.0 in R (Rabosky et al., 2014).

282 *Lineage diversification rate analyses*

I performed analyses of origination and extinction rates in hominoid and cercopithecoid fossil records to examine the correspondence between lineage diversification and the patterns in disparification emphasized in the analyses of morphological rates and mosaicism. Fossil occurrence data spanning primates were acquired from the Paleobiology Database (paleobiodb.org) on July 31, 2019. This dataset was partitioned into two subsets: one encompassing Hominoidea and the other representing Cercopithecoidea. Rates of origination and extinction were inferred from each subset separately using PyRate (Silvestero et al. 2014). The inferential model was constrained to contain uniform origination and extinction rates across time, thus ignoring the possibility of diversification shifts within each clade. Preservation was constrained to being time-homogeneous and was assumed to be uniform within each clade. While ignoring potential information regarding diversification rate heterogeneity through time, this simplified model matches classic paleobiological work that assumes simple birth-death-sampling models and was therefore appropriate for the sister clade comparison of average diversification rates while avoiding possible model overfitting that may obfuscate the straightforward test sought here.

*Simulated Markovian diffusion*

To examine the expected effect of constructional opportunity stemming from both developmental and functional constraint on phenotypic evolution, I designed a set of evolutionary simulations based on a simple Markovian diffusion. In this system, quantitative traits belonging to a single population of organisms evolve stochastically along a fitness landscape. Each generation, values for each trait are proposed. Values that

increase the overall fitness of the population are accepted. To mimic the effect of drift, values that decrease fitness are also accepted with some (user-specified) probability. Developmental constraint can be mimicked by proposing values for traits that covary, while functional constraints are modeled by evolving traits along a shared, multivariate adaptive landscape, modelled here using a mixture of multivariate Gaussian distributions. In a completely unconstrained system, each trait is evolved according to its own univariate landscape, with its value drawn independently of all others in each generation. Performing simulations in this way facilitated an illustration of the potential for functional and developmental integration to constrain evolutionary rates in an adaptive landscape. Although distinguishing between these modes of integration is generally difficult or impossible in paleontological study systems, the simulations performed here provide insight by testing 1) the potential for varying systems of integration to catalyze or constrain adaptive change and 2) the extent to which functional and developmental integration generate overlapping and distinct patterns in evolutionary rate and disparity. When placed in a macroevolutionary context, the simulations here should be thought of a demonstration of the possible microevolutionary processes that may have driven the higher-level patterns in evolutionary rate occurring along a single phylogenetic branch in the mosaic analyses. The script used to generate these simulations is available in the data supplement.

## Results and Discussion

### *Strength of integration throughout the haplorrhine radiation*

Calculating character correlations from the skeletal data and PICs at each internal node in the extant haplorrhine phylogeny revealed two episodes of reduced integration (Fig. 2). The first occurred at the root of Hominoidea, where the correlation decreased from -0.21 at the ancestor of catarrhines, to -0.06 at the root of hominoids. The second episode occurred in the ancestor of chimpanzees and humans, decreasing from 0.09 to 0.02. This show that the reduction in integration across apes between the fore- and hindlimbs revealed by Young and colleagues (2009) extends across the skeleton. In contrast, both cercopithecoids (0.24 correlation) and platyrrhines (0.16 correlation) display substantially higher integration than was observed in any of the ape hypothetical ancestors.

*Composition of mosaic suites*

The analysis of mosaic disparity recovered five suites of traits (Fig 3a). The cranium was the largest contributor of both traits and variance across all suites except for C4, which was represented by the pelvis alone (Fig. 3b and 3c). This reflects the higher sampling of cranial traits in the dataset. While the cranium has previously been shown to display substantial modularity (Felice and Goswami 2017), the results here suggest that individual cranial modules may result from the formation of broader evolutionary complexes shared with the post-cranium. The suites were distinct in their composition across postcranial anatomy: C0 was represented strongly by the wrist, ulna, and humerus; C1 was represented postcranially by the scapula; C2 by wrist and pelvic traits. The cranium was represented even more strongly than expected in C3 and contributed nearly half of the variance (Fig. 3b).

348 *Rates of morphological evolution*

349 The phylogenetic rate calculations for each suite revealed a strong pattern of
350 evolutionary mosaicism (Fig. 3a). Three of the suites, C0, C1, and C3, displayed the
351 highest rates after the divergence of the great apes from hylobatids, but before the
352 divergence of gorillas from humans and chimpanzees. The two suites that did not
353 experience the shared great ape rate increase, C2 and C4, experienced large bursts in
354 *Homo*. This finding is consistent with general knowledge of human evolution, as both
355 suites are dominated by cranial traits and pelvic traits related to birthing and locomotor
356 function (Table S1).

357 The rate analyses show that humans have experienced major macroevolutionary
358 bursts. However, these are built over an anatomical structure shared by all great apes that
359 was shaped in the Miocene during similarly dramatic episodes. For example, although
360 suite C0 increased in evolutionary rate along the human branch, its evolution was shaped
361 by a sustained period of elevated rate between 20 and 10 million years ago. This suggests
362 that much of the 'groundwork' underlying the derivation of humans' unique features may
363 predate the divergence between our lineage and chimpanzees'. The mosaic analysis also
364 demonstrates that substantial visible phenotypic novelty can result from the evolutionary
365 remodeling of a small subset of the anatomy. The most elevated evolutionary rates in
366 humans were observed in suites C2, C3, and C4, which cumulatively comprise fewer than
367 one-third of the traits sampled in the matrix (Table S1). C4, the smallest suite (10 traits)
368 displayed by far the largest increase in rate along the *Homo* lineage. Perhaps notably, C4
369 also was the most static character suite throughout the earlier stages in the hominoid

radiation. Although enumerating characters does not itself constitute a particularly compelling independent line of evidence from which to interpret macroevolutionary trends, the mosaic pattern recovered here does suggest that the subset of biological variation unique to the human body plan is fairly small in comparison to the wide spectrum of evolutionary variance accumulated throughout ape evolution.

While the large amounts of missing data among the fossil taxa made an additional mosaic analysis infeasible, their inclusion revealed an otherwise hidden shift in evolutionary rate that occurred at the root of hominoidea (approximately 30 million years ago). The fossil data also recapitulated the burst in evolutionary rate during the mid-Miocene that was displayed by C0 and C1 in the mosaic analysis (Fig. 3 and 4). When averaging over all the traits and including fossil taxa, these two episodes are the most dramatic macroevolutionary events when tracing the evolutionary lineage leading to *Homo*, suggesting the importance of early shifts in the ape body plan in shaping the functional morphologies of living taxa.

*Rates of neurological evolution*

As with morphology, all great apes appear to have differentiated rapidly from other catarrhines in both EQ and ED. *Homo* displays the highest rate of both EQ and ED evolution. However, the human rate shift in both traits occurred as part of an older trend of rapid neurological evolution in African apes. For EQ, humans experienced a substantial increase in evolutionary rate relative to the rest of the African apes, despite the statistical evidence for a shared rate shift at the root of the clade (Fig. 5b). The shared macroevolutionary regime shared by all African apes is most apparent in encephalization

development (Fig. 5a), where the estimated evolutionary rate in *Homo* increased only slightly after splitting from *Pan* (Fig. 5c). It appears that the increased encephalization developed throughout the post-natal period in humans reflects a general trend among great apes in the evolutionary plasticity of neurological development. As a result, the ability to develop a relatively large mass of brain tissue does not itself appear to be a strong limiting factor in the evolution of large encephalization in humans. Instead, the morphological analyses suggest that pelvic traits (C4 in Fig. 1) may have demanded a more dramatic alteration in macroevolutionary regime.

*Structural and ecological opportunity in ape evolution*

The elevated evolutionary rates experienced by apes early in their divergence appear to correspond to a general relaxation of constraint in early Miocene stem and ancestral hominoids. The reduction in integration across the skeleton and burst in the evolutionary rate of neurological development that occur at the base of the hominoid clade correspond in timing to the elevated rates in morphological evolution observed in most of the skeletal characters examined here (Fig. 3 and 4). Freed from previous functional and developmental limitations, ape body plans would have rapidly diversified when placed in the context of the repeated environmental fluctuations that occurred throughout the mid and late Miocene (Michel et al. 2014, Hunt 2016) before becoming functionally canalized through development and stabilizing selection. This pattern is consistent with a scenario in which morphological features evolve by stochastic diffusion on a Simpsonian adaptive landscape that is alternately dampened and released by relaxed and shifting patterns in character integration.

414 Rapid and frequent environmental fluctuations throughout the Miocene suggest an
415 abundance of theoretically available adaptive zones during the evolution of both
416 cercopithecoids and hominoids. Paleoecological information extracted from deposits
417 containing key hominoid taxa are so variable that environmental turnover often outpaces
418 the effects of time-averaging (Michel et al. 2014). Early Miocene ape and monkey
419 species evolved in often overlapping environmental conditions and shared similar
420 ecomorphological and dietary habits. However, as their lineages diverged, apes evolved a
421 diverse set of locomotor suites, while evolution in locomotor features has remained
422 comparatively static across old world monkeys (Hunt 2016). The patterns in
423 developmental and mosaic morphological evolution revealed here suggest that the
424 substantial differences between the two taxa in phenotypic disparity were shaped more by
425 differences in patterns in integration and constraint rather than from the ecological
426 opportunities available to either. While hominoids and cercopithecoids inhabited a
427 similar range of habitats throughout their evolution, and so likely experienced a similar
428 abundance of ecological opportunity, greater constructional opportunity is a
429 distinguishing feature that correlates with hominoids' vast disparity in skeletal
430 morphology.
431 The scenario entertained here for apes is consistent with recent work that suggests
432 that the initial burst in phenotypic disparity that often accompanies the origin of a new
433 lineage can result from an early relaxation of constraints through the dissolution of
434 integrated modules that is followed by reformation of character suites that lead to rapid,
435 correlated evolutionary changes between constituent characters (Wagner 2018). In the

436 cited work, the author distinguishes this 'breakup-relinkage' model with one where
437 evolutionary rates are elevated by a relaxation of constraint alone. Although in this study,
438 I have focused most of the discussion on the relaxation of constraints, the formation of
439 mosaic character suites and their distinct evolutionary patterns imply a strong pattern of
440 integration within apes. This is reflected in the ancestral correlation patterns, which show
441 that an initial decrease in integration at the root of hominoids was followed by an
442 increase at the following node (Fig. 2). Therefore, the recanalization of functional
443 variation into a set of suites with distinct functional and developmental properties early in
444 hominoid variation is likely equally important to the initial relaxation in constraint in
445 having driven the remarkable morphological disparity observed across hominoid species.

446 *"Preadaptation" and developmental enablers in apes*

447 Bursts in phenotypic change and diversification are often preceded by
448 evolutionary enablers that facilitate the construction of more diverse morphological forms
449 or fulfill a necessary condition for the later emergence of a more derived trait. Such
450 patterns have been suggested to stem from higher-level processes variously referred to as
451 "preadaptation" (Bock 1959), "exaptation" (Gould and Vrba 1982), and "developmental
452 enablement" (Donoghue 2005). The evolution of developmental, morphological, and
453 behavioral traits is often hierarchical through functional inter-dependencies and
454 temporally autocorrelated, with changes in traits at relatively lower levels 'setting the
455 stage' for higher-level traits by providing the developmental or structural conditions
456 necessary for their emergence. The stepwise macroevolutionary bursts observed here
457 show that hominoid evolution has been defined by sequential, episodic releases in

458 constraint that likely set the stage for later innovations that compounded upon earlier
459 rearrangements in the structure of developmental and functional integration.

460 The related concepts of preadaptation, exaptation, and developmental enablement
461 all focus on identifying the origin of single characters that facilitate the later emergence
462 of more derived states. However, the patterns presented here suggest that such processes
463 may often be better characterized as reflecting larger changes in developmental and
464 functional character-linkage systems rather than by the sequential derivation of individual
465 characters. The dramatic bursts in evolutionary rate that occur in the largest character
466 suites coincide with or immediately follow the reduction in integration that occurred at
467 the root of hominoids. This suggests that a general shift in functional and/or
468 developmental integration occurred near this time. This shift precedes and, although
469 speculative, may have resulted in a general predisposition across apes that facilitated the
470 later functional divergence of later species into an unusually broad range of habits.
471 Therefore, rather than stemming from a single "preadaptive" character, the morphological
472 disparity of apes and the emergence of features derived in single lineages (such as
473 bipedalism in humans) may be better explained by a shift in developmental and
474 functional integration patterns earlier in ape evolution.

475 To provide a specific example, the effect of the enhanced evolvability conferred
476 by reduced integration appears to have contributed to the emergence of key human traits.
477 Suites C2 and C3 from the morphological analysis, represented disproportionately by the
478 cranium and pelvis, experienced an initial burst in evolutionary rate along the branch
479 leading to humans and chimpanzees. This was then followed by dramatic bursts in *Homo*

480 (Fig. 3). Likewise, EQ and ED have been evolving rapidly throughout the ape radiation,
481 with ED experiencing an initial increase in evolutionary rate before the splitting of
482 gorillas, chimps, and humans followed by more dramatic upticks of rate in humans in
483 both traits (Fig. 5c). The occurrence of evolutionary rate shifts in traits important to
484 humans earlier in the great ape clade reflects the increased evolvability shared by all
485 apes. In addition, comparison of the human-specific evolutionary rates in cranial, pelvic,
486 and neurological traits to the varying strength of skeletal integration throughout hominoid
487 evolution show that the elevated rates in humans were immediately preceded by a
488 substantial decrease in constraint, recapitulating a similar pattern to the co-occurring
489 shifts in evolutionary rate and integration earlier in ape evolution. This result provides
490 independent evidence of the "preadaptive" potency of shifts in integration in promoting
491 rapid and dramatic evolutionary remodeling of morphology.

492 Although demanding more detailed exploration with more resolute data, it is
493 possible that the initial bursts in ED and suite C2 and C3 evolution, coupled with the
494 reduced integration at the ancestor of chimp and humans, may reflect a set of structural
495 rearrangements that facilitated, at least in part, the later emergence of human-specific
496 neurological and cognitive features. This scenario echoes the results of Rice (1998), who
497 demonstrated that humans and chimpanzees, to the exclusion of gorillas, both inherited a
498 shared 'additional' stage of brain development from our most recent common ancestor. It
499 is therefore possible that chimpazees possess more of the neurological and cranial
500 groundwork that contributed to the evolution of humans' particular mode of cognition
501 than has previously been appreciated.

The patterns uncovered here suggest that many evolutionary studies focusing on preadapation and exaptation would benefit by shifting focus from individual features to patterns in integration and modularity across broad suites of characters. Although the concept is essentially unchanged as applied to integration patterns, it may be more accurate in the example here to refer instead to an 'evolutionary predisposition' given the lack of evidence for a specific sequence of selective regimes (Smith et al. 2018). This semantic argument is likely also valid in more traditional examples of single trait exaptations or preadaptations. And so, a generalization from preadaptation or exaptation to evolutionary predisposition that 1) incorporates integration patterns and 2) shifts emphasis from adaptation, which makes assumptions about the (often unknowable) set of historical microevolutionary processes, to the sequence of observable states in both characters and integration patterns can provide a stronger conceptual basis for future work that considers contingency and sequential order in the evolutionary pathways of complex traits. Although this reconceptualization might superficially appear to de-emphasize evolutionary process in favor of pattern, I would instead argue that constraining the scale of inquiry and incorporating a broader range of biological complexity can facilitate the reconstruction of elusive higher-level macroevolutionary processes that shape organismal diversification and disparification over deep timescales. This formulation also avoids the conceptual and practical frustrations that occur when attempting to invoke the concepts of preadaptation and exaptation to explain evolutionary history over deep timescales by reducing dependency on knowledge of lower-level population processes.

524 *Diversification and disparification in haplorrhine evolution*

525 Cercopithecoids have diversified at over twice the rate as hominoids over the
526 same time scale (Table 1). One limitation of these analyses stems from cercopithecoids'
527 somewhat poor fossil record as compared to hominoids. Nevertheless, the difference in
528 preservation rates estimated in each clade (~3 in apes compared to ~2.6 in
529 cercopithecoids) should ameliorate some of the potential effect of this bias on parameter
530 estimates. The general pattern of higher net diversification in cercopithecoids is also
531 consistent with previous neontological results (Purvis et al. 1995), suggesting that the
532 paleontological estimates presented here are adequately robust to these effects. This
533 difference in lineage diversification rates between both taxa demonstrates that increased
534 morphological disparification is, overall, not correlated with faster lineage diversification
535 in haplorrhine primates. While the evolutionary predisposition conferred upon apes by
536 their relaxed integration corresponds to an increase in morphological disparity, this effect
537 does not extend to lineage diversity.

538 On the surface, the overall similarity in the environments, dietary niches, and
539 geographical ranges of hominoids and cercopithecoids suggests that cercopithecoids have
540 a selective advantage in the species-sorting dynamics between the two clades. However,
541 the long-term persistence of hominoids and their remarkable innovation in locomotor
542 function relative to cercopithecoids throughout this timespan suggests an equilibrium in
543 their relative abundances (Van Valen 1975, Chesson 2000). Although cercopithecoids
544 experienced less disparification in postcranial morphology, they display a broader range
545 of derived digestive physiologies, including both intestinal and dental features, associated

546 with food processing (Hunt 2016). Given these observations, it is possible that the
547 differential in diversification rate between cercopithecoids and hominoids stems from
548 differences in the timescales of their life histories and other factors not directly related to
549 interspecific competitive ability. If this is the case, hominoids may achieve steady
550 persistence through higher evolvability conferred by reduced integration and increased
551 developmental flexibility when faced with changing environments, while cercopithecoids
552 may do so through a combination of their higher net diversification rates and capability to
553 exploit a range of dietary resources through their digestive physiologies. Such differences
554 would be consistent with an equilibrium model of coexistence rather than a simple
555 species selection model that predicts the ultimate extinction of hominoids through
556 competitive exclusion by cercopithecoids. Nevertheless, more rigorous comparison of
557 each of these attributes in both lineages is needed to further constrain the range of
558 possible explanatory factors.

559 *Constrained Markovian diffusion and entropy*

560 The patterns in character disparity shown here evoke a Markovian diffusion that is
561 dampened by constraint. The tightly integrated nature of vertebrate body plans suggests
562 major constraints in their ability to fill morphospace. However, the pattern displayed by
563 apes suggests that the structure of integration may sometimes shift, allowing diffusion
564 into new areas. Morphological evolution might then be conceived as a multivariate
565 diffusion in morphospace where movement is directionally biased due to fitness
566 differences modelled by a traditional Simpsonian adaptive landscape and certain regions
567 are rendered inaccessible by structural interactions between characters. Although this

568 diffusive model, including the feedback links between phenotype, development, and
569 environment, has been considered previously (Fisher 1986), its behavior has not been
570 well explored in this context.

571 The Monte Carlo simulations presented here provide a theoretical illustration of
572 the population-level dynamics stemming from one possible set of integration scenarios
573 and their potential effects on the evolutionary disparity/rate along a single branch in
574 Figures 3 or 4. The results shed light on the empirical analyses by demonstrating the
575 overlapping and distinct empirical patterns that can result from varying levels of
576 developmental and functional integration in a simple closed system in the absence of
577 environmental fluctuation (Fig. 6). As is expected from quantitative genetic theory
578 (Cheverud 1984, Maynard-Smith et al. 1985), developmental and functional constraints
579 can generate similar patterns (Fig. 6a and 6b). In all these cases, the overall entropy
580 observed in the system over time remains low, with the system tending to become stuck
581 or moving away very slowly from a suboptimal location (Fig 4c and 4e) or crawling
582 slowly in concert along a gradient (Fig 6a and 6b). However, when both types of
583 constraint are released, the system displays high entropy, with each trait able to
584 independently jump between peaks (Fig. 6d). Such unconstrained movement would be
585 expected to result in higher phenotypic disparity over macroevolutionary timescales by
586 freeing individual lineages to generate novel character combinations when exposed to
587 distinct and changing environments.

588 The patterns in increased evolutionary rate and entropy across traits displayed by
589 the less constrained simulated diffusions provide mechanistic explanations that are

590 consistent with the bursts in evolutionary rate encountered throughout hominoid
591 evolution. Although it is not possible in the empirical example to distinguish between
592 functional and developmental integration as is done in the simulations, the general pattern
593 of reduced integration that gives way to increased evolutionary rate is consistent between
594 the two. Alternation between the varying strengths of integration as explored in the
595 simulations would likely generate substantial novelty during periods of relaxed
596 integration. Episodes of reduced developmental constraint (Figs. 2 and 5a) may have
597 generated an initial burst of constructional opportunity that lead to rapid morphological
598 diversification as ape populations were exposed to highly variable environments
599 throughout the mid-Miocene. If the processes modelled in the simulations drove the
600 patterns revealed in the empirical analyses, this sequence of events would represent true
601 preadaptation in the sense that relaxed integration leads to increased mean population
602 fitness. Under the evolutionary models explored here and elsewhere (Wagner 2018),
603 stabilizing effects such as developmental canalization (Waddington 1959) or functional
604 covariance (Cheverud 1984) would then be expected to re-constrain the newly divergent
605 phenotypes after an initial burst in disparification. This dampened diffusive model was
606 explored in early work in theoretical morphology that focused on the constrained filling
607 of morphospace (Raup 1968).

608 The simulated diffusions and empirical pattern in evolutionary predisposition
609 revealed here hint at the source of teleological concepts in human evolution. If the
610 morphological and neurological traits can be assumed to have followed a multivariate
611 Markovian diffusion that is at least qualitatively similar to the simulations in Figure 6

612 (especially Fig. 6a), the pattern in evolutionary rates along the path leading to humans
613 may paint a misleading view that such changes have followed a progressive trend leading
614 to a human-defined apex. However, the mosaic analysis here suggests that humans'
615 biological uniqueness can be attributed to a relatively small number of anatomical
616 rearrangements built over a longer diffusion into an area of developmental-morphospace
617 occupied by all apes that is characterized by increased structural opportunity. Instead of
618 treating humans as exceptional, this view suggests that the structural opportunities that
619 emerged early in ape evolution may have freed the ancestors of currently extant taxa to
620 blaze unique trajectories along a complex, multivariate adaptive landscape that would
621 have been otherwise inaccessible. Structurally, all ape species might therefore be viewed
622 as equally progressive in their evolution, with species-level differences in form and
623 function shaped by stochastic differences in separate realized evolutionary paths along a
624 shared adaptive landscape. Alternatively, separate taxa may have forged new and unique
625 adaptive landscapes following speciation events as structural differences between newly
626 isolated species drove the creation of new functional niches early in hominoid evolution.
627 The empirical and simulated analyses presented here are consistent with, although
628 do not provide independent support for, a picture of morphological evolution that
629 involves episodic diffusion across adaptive zones. However, the empirical and theoretical
630 analyses allow for alternating and interacting roles for both ecological and constructional
631 opportunity. This view can supplement many existing conceptions of adaptive radiation
632 and key innovation by providing an alternative to ecological opportunity as a lone driving
633 factor in the disparification of form. Instead, phenotypic disparity produced through

634 diffusion into a set of abundant adaptive zones can be directed and limited by the
635 availability of structural opportunity. Nature surely merges these simplified extremes
636 when shaping patterns in biodiversity (Seilacher 1991), and so increased emphasis on the
637 interplay between ecological, developmental, and constructional factors will be a critical
638 part of shaping a pluralistic understanding of the complex patterns and processes that
639 have shaped the vast diversity across the tree of life.
640
641
642
643
644
645
646
647
648
649
650
651
652
653
654
655

## References

Andrews P. 1992 Evolution and environment in the Hominoidea. Nature 360, 641–646. (doi:10.1038/360641a0)

Berge C. 1998 Heterochronic processes in human evolution: An ontogenetic analysis of the hominid pelvis. American Journal of Physical Anthropology 105, 441–459. (doi:10.1002/(sici)1096-8644(199804)105:4<441::aid-ajpa4>3.0.co;2-r)

Bock J. 1959 Preadaptation and multiple evolutionary pathways. Evolution 13, 194-211.

Boddy AM, McGowen MR, Sherwood CC, Grossman LI, Goodman M, Wildman DE. 2012 Comparative analysis of encephalization in mammals reveals relaxed constraints on anthropoid primate and cetacean brain scaling. Journal of Evolutionary Biology 25, 981–994. (doi:10.1111/j.1420-9101.2012.02491.x)

Bouckaert R, Heled J, Kühnert D, Vaughan T, Wu C-H, Xie D, Suchard MA, Rambaut A, Drummond AJ. 2014 BEAST 2: A Software Platform for Bayesian Evolutionary Analysis. PLoS Computational Biology 10, e1003537. (doi:10.1371/journal.pcbi.1003537)

Capellini I, Venditti C, Barton, RA. 2010 Phylogeny and metabolic scaling in mammals. Ecology, 91, 2783-2793.

Charlesworth B, Lande R, Slatkin M. 1982 A Neo-Darwinian Commentary on Macroevolution. Evolution 36, 474–498. (doi:10.1111/j.1558-5646.1982.tb05068.x)

Chesson P. 2000 Mechanisms of maintenance of species diversity. Annual Review of Ecology and Systematics, 31, 343-366.

678 Cheverud JM. 1984 Quantitative genetics and developmental constraints on evolution by
679 selection. Journal of Theoretical Biology 110, 155–171. (doi:10.1016/s0022-
680 5193(84)80050-8)
681 Crouch NMA, Ricklefs RE. 2019 Speciation Rate Is Independent of the Rate of
682 Evolution of Morphological Size, Shape, and Absolute Morphological
683 Specialization in a Large Clade of Birds. The American Naturalist 193, E78–E91.
684 (doi:10.1086/701630)
685 Donoghue MJ, Ree RH. 2000 Homoplasy and Developmental Constraint: A Model and
686 an Example from Plants. American Zoologist 40, 759–769.
687 (doi:10.1093/icb/40.5.759)
688 Donoghue MJ. 2005 Key innovations, convergence, and success: macroevolutionary
689 lessons from plant phylogeny. Paleobiology 31, 77-93. (doi: 10.1666/0094-
690 8373(2005)031[0077:KICASM]2.0.CO;2)
691 Felice RN, Goswami A. 2017 Developmental origins of mosaic evolution in the avian
692 cranium. Proceedings of the National Academy of Sciences 115, 555–560.
693 (doi:10.1073/pnas.1716437115)
694 Felsenstein J. 1985 Phylogenies and the comparative method. The American Naturalist,
695 125, 1-15.
696 Fisher, DC. 1986 Progress in organismal design. Pp. 99-117 in: Patterns and Processes in
697 the History of Life. Raup DM and Jablonski D, eds. Springer, Berlin, Heidelberg.
698 Goswami A, Binder WJ, Meachen J, O'Keefe FR. 2015 The fossil record of phenotypic
699 integration and modularity: A deep-time perspective on developmental and

700 evolutionary dynamics. Proceedings of the National Academy of Sciences 112,
701 4891–4896. (doi:10.1073/pnas.1403667112)
702 Goswami A, Smaers JB, Soligo C, Polly PD. 2014 The macroevolutionary consequences
703 of phenotypic integration: from development to deep time. Philosophical
704 Transactions of the Royal Society B: Biological Sciences 369, 20130254–
705 20130254. (doi:10.1098/rstb.2013.0254)
706 Gould SJ, Vrba ES. 1982 Exaptation—a Missing Term in the Science of Form.
707 Paleobiology 8, 4–15. (doi:10.1017/s0094837300004310)
708 Gould SJ and Lewontin RC. 1979 The spandrels of San Marco and the Panglossian
709 paradigm: a critique of the adaptationist programme. Proceedings of the Royal
710 Society of London. Series B. Biological Sciences 205, 581–598.
711 (doi:10.1098/rspb.1979.0086)
712 Gould, SJ. 1977 Ontogeny and Phylogeny. Harvard University Press, Cambridge, USA.
713 Harmon LJ. 2003 Tempo and Mode of Evolutionary Radiation in Iguanian Lizards.
714 Science 301, 961–964. (doi:10.1126/science.1084786)
715 Holloway RL. 1973 Endocranial volumes of early African hominids, and the role of the
716 brain in human mosaic evolution. Journal of Human Evolution 2, 449–459.
717 (doi:10.1016/0047-2484(73)90123-1)
718 Hunt KD. 2016 Why are there apes? Evidence for the co-evolution of ape and monkey
719 ecomorphology. Journal of Anatomy 228, 630–685. (doi:10.1111/joa.12454)
720 Lewton KL. 2010 Locomotor function and the evolution of the primate pelvis. (Doctoral
721 dissertation, Arizona State University).

722 Losos JB. 2010 Adaptive Radiation, Ecological Opportunity, and Evolutionary
723 Determinism. The American Naturalist 175, 623–639. (doi:10.1086/652433)
724 Mahler DL, Ingram T, Revell LJ, Losos JB. 2013 Exceptional Convergence on the
725 Macroevolutionary Landscape in Island Lizard Radiations. Science 341, 292–295.
726 (doi:10.1126/science.1232392)
727 McHenry H. 1975 Fossils and the mosaic nature of human evolution. Science 190, 425–
728 431. (doi:10.1126/science.809842)
729 Michel LA et al. 2014 Remnants of an ancient forest provide ecological context for Early
730 Miocene fossil apes. Nature Communications 5. (doi:10.1038/ncomms4236)
731 Rice, SH. 2002. The role of heterochrony in primate brain evolution. In: Human
732 evolution through developmental change. N. Minugh-Purvis & K.J. McNamara,
733 eds. Johns Hopkins Univ. Press, Baltimore.
734 Seilacher A. 1991 Self-Organizing Mechanisms in Morphogenesis and Evolution. In
735 Constructional Morphology and Evolution, pp. 251–271. Springer Berlin
736 Heidelberg. (doi:10.1007/978-3-642-76156-0_17)
737 Silvestro D, Salamin N, Schnitzler J. 2014 PyRate: a new program to estimate speciation
738 and extinction rates from incomplete fossil data. Methods in Ecology and
739 Evolution 5, 1126-1131.
740 Smith JM, Burian R, Kauffman S, Alberch P, Campbell J, Goodwin B, Lande R, Raup D,
741 Wolpert L. 1985 Developmental Constraints and Evolution: A Perspective from
742 the Mountain Lake Conference on Development and Evolution. The Quarterly
743 Review of Biology 60, 265–287. (doi:10.1086/414425)

744 Smith SA, Brown JW, Yang Y, Bruenn R, Drummond CP, Brockington SF, Walker JF,
745 Last N, Douglas N, Moore MJ. 2018 Disparity, Diversity, and Duplications in the
746 Caryophyllales. New Phytologist 217, 836-854.
747 Olson ME. 2012 The developmental renaissance in adaptationism. Trends in Ecology and
748 Evolution 27, 278–287. (doi:10.1016/j.tree.2011.12.005)
749 Olson EC and Miller RL. 1958. Morphological Integration. University of Chicago Press.
750 Parins-Fukuchi C. 2018 Bayesian placement of fossils on phylogenies using quantitative
751 morphometric data. Evolution 72, 1801–1814. (doi:10.1111/evo.13516)
752 Parins-Fukuchi C. 2019 Detecting mosaic patterns in macroevolutionary disparity.
753 *bioRxiv*, 423228.
754 Purvis A, Nee S, Harvey PH. 1995 Macroevolutionary inferences from primate
755 phylogeny. Proceedings of the Royal Society of London, Series B: Biological
756 Sciences 260, 329-333.
757 Rabosky DL, Santini F, Eastman J, Smith SA, Sidlauskas B, Chang J, Alfaro ME. 2013
758 Rates of speciation and morphological evolution are correlated across the largest
759 vertebrate radiation. Nature Communications 4. (doi:10.1038/ncomms2958)
760 Rabosky DL. 2014 Automatic Detection of Key Innovations, Rate Shifts, and Diversity-
761 Dependence on Phylogenetic Trees. PLoS One 9, e89543.
762 (doi:10.1371/journal.pone.0089543)
763 Rabosky DL, Grundler M, Anderson C, Title P, Shi JJ, Brown JW, Huang H, Larson JG.
764 2014 BAMMtools: an R package for the analysis of evolutionary dynamics on

765 phylogenetic trees. Methods in Ecology and Evolution 5, 701–707.
766 (doi:10.1111/2041-210x.12199)
767 Rainey PB, Travisano M. 1998 Adaptive radiation in a heterogeneous environment.
768 Nature 394, 69–72. (doi:10.1038/27900)
769 Raup, DM. 1966 Geometric analysis of shell coiling: general problems. Journal of
770 Paleontology, 1178-1190.
771 Raup DM. 1968 Theoretical morphology of echinoid growth. Journal of Paleontology 42,
772 50-63.
773 Ruff CB. 1994 Morphological adaptation to climate in modern and fossil hominids.
774 American Journal of Physical Anthropology 37, 65–107.
775 (doi:10.1002/ajpa.1330370605)
776 Simpson GG. 1944 Tempo and Mode in Evolution. Columbia University Press. New
777 York.
778 Slater GJ, Friscia AR. 2019 Hierarchy in adaptive radiation: A case study using the
779 Carnivora (Mammalia). Evolution 73, 524–539. (doi:10.1111/evo.13689)
780 Slater GJ. 2015 Iterative adaptive radiations of fossil canids show no evidence for
781 diversity-dependent trait evolution. Proceedings of the National Academy of
782 Sciences 112, 4897–4902. (doi:10.1073/pnas.1403666111)
783 Sukumaran J, Holder MT. 2010 DendroPy: a Python library for phylogenetic computing.
784 Bioinformatics 26, 1569–1571. (doi:10.1093/bioinformatics/btq228)
785 Stebbins GL. 1983 Mosaic evolution: An integrating principle for the modern synthesis.
786 Experientia 39, 823–834. (doi:10.1007/bf01990398)

787 Stebbins GL. 1984 Mosaic evolution, mosaic selection and angiosperm phylogeny.
788 Botanical Journal of the Linnean Society 88, 149–164. (doi:10.1111/j.1095-
789 8339.1984.tb01568.x)
790 Turing AM. 1953 The chemical basis of morphogenesis. Philosophical Transactions of
791 the Royal Society (part B) 237, 37-72.
792 Van Valen L. 1975 Group selection, sex, and fossils. Evolution, 29, 87-94.
793 Vos RA. 2006 Inferring large phylogenies: the big tree problem (Doctoral dissertation,
794 Simon Fraser University)
795 Waddington CH. 1959 Canalization of Development and Genetic Assimilation of
796 Acquired Characters. Nature 183, 1654–1655. (doi:10.1038/1831654a0)
797 Wagner CE, Harmon LJ, Seehausen O. 2012 Ecological opportunity and sexual selection
798 together predict adaptive radiation. Nature 487, 366–369.
799 (doi:10.1038/nature11144)
800 Wagner GP, Pavlicev M, Cheverud JM. 2007 The road to modularity. Nature Reviews
801 Genetics 8, 921-931.
802 Wagner GP, Amemiya C, Ruddle F. 2003 Hox cluster duplications and the opportunity
803 for evolutionary novelties. Proceedings of the National Academy of Sciences 100,
804 14603–14606. (doi:10.1073/pnas.2536656100)
805 Wagner GP. 1988 The influence of variation and of developmental constraints on the rate
806 of multivariate phenotypic evolution. Journal of Evolutionary Biology 1, 45–66.
807 (doi:10.1046/j.1420-9101.1988.1010045.x)

808 Wagner PJ. 2018 Early bursts of disparity and the reorganization of character integration.
809 Proceedings of the Royal Society B: Biological Sciences 285, 20181604.
810 (doi:10.1098/rspb.2018.1604)
811 Worthington S. 2012 New approaches to late Miocene hominoid systematics: Ranking
812 morphological characters by phylogenetic signal (Doctoral dissertation, New
813 York University).
814 Yoder JB, et al. 2010 Ecological opportunity and the origin of adaptive radiations.
815 Journal of Evolutionary Biology 23, 1581–1596. (doi:10.1111/j.1420-
816 9101.2010.02029.x)
817 Young NM, Wagner GP, Hallgrímsson B. 2010 Development and the evolvability of
818 human limbs. Proceedings of the National Academy of Sciences 107, 3400–3405.
819 (doi:10.1073/pnas.0911856107)
820
821
822
823
824
825
826
827
828
829

## Tables

| Clade | Origination | Extinction | Net diversification | Preservation |
|---|---|---|---|---|
| Hominoidea | 0.395 | 0.338 | 0.057 | 3.121 |
| Cercopithecoidea | 0.251 | 0.128 | 0.123 | 2.551 |

*Table 1.* Lineage diversification and preservation rate parameters estimated in apes (Hominoidea) and Old World monkeys (Cercopithecoids). Parameters were summarized as the mean values from four million Markov-Chain Monte Carlo generations after discarding 20% as burn-in.

# Figures

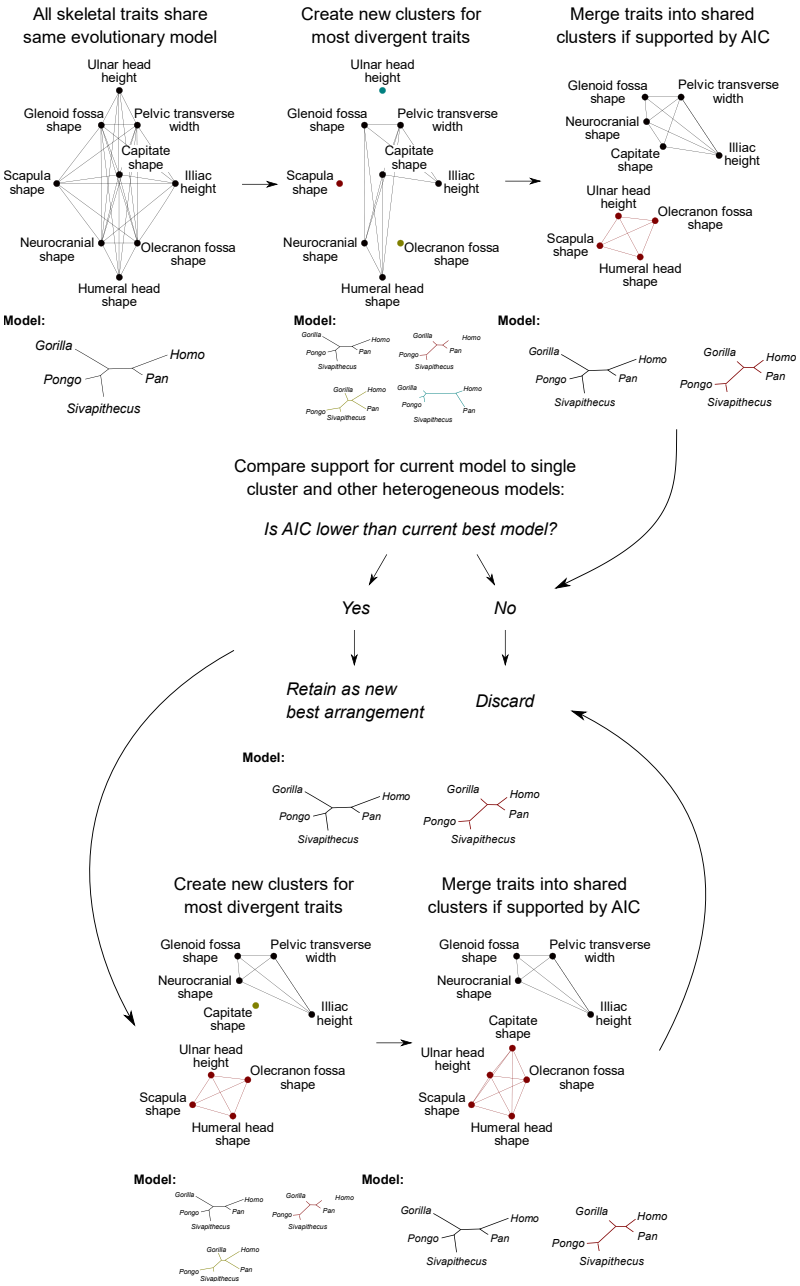


*Figure 1*. The mosaic inference procedure starts by modelling all characters under a unified phylogenetic model. The algorithm then splits traits with divergent patterns in disparity into their own suites and then greedily merges these suite fragments until the AIC score ceases to improve. The splitting and merging steps are then alternated until the

855 AIC scores of the final merged models cease to improve. The best clustering achieved
856 from this procedure represents the best-supported heterogeneous model of character
857 integration.

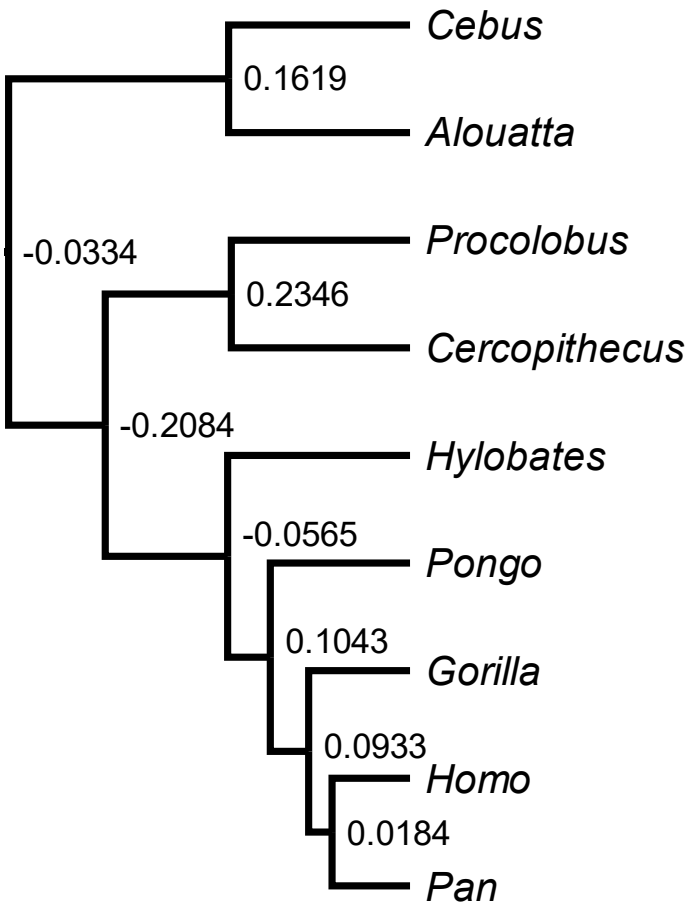


858

859 *Figure 2*. Strength of integration across catarrhine evolution. Node labels correspond to
860 the strength and polarity of correlation in the traits or phylogenetic independent contrasts
861 (PICs) at each subtending node, depending on whether the child was a tip (traits) or
862 internal node (PICs). Higher correlations in either direction (closer to either 1 or -1)
863 indicate higher integration, while lower correlations (closer to 0) indicate weaker
864 integration.

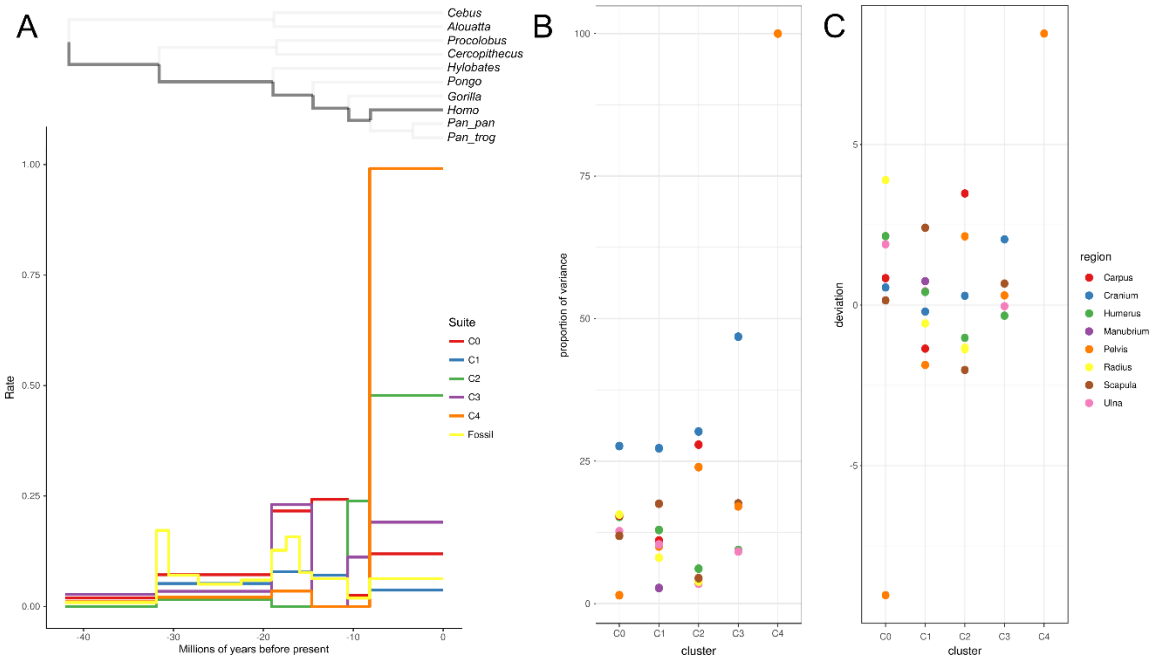


865

866 *Figure 3.* A) Mosaic evolutionary rates calculated while walking back from *Homo* to the

867 last common ancestor of New World monkeys, Old World Monkeys, and apes. B)

868 Variance contributed to each suite by each skeletal region, estimated from a principal

869 component analysis. C) Skeletal regions over-represented in each mosaic evolutionary

870 suite. Values above zero correspond to regions that occupy a higher proportion of their

871 clusters than expected.

872

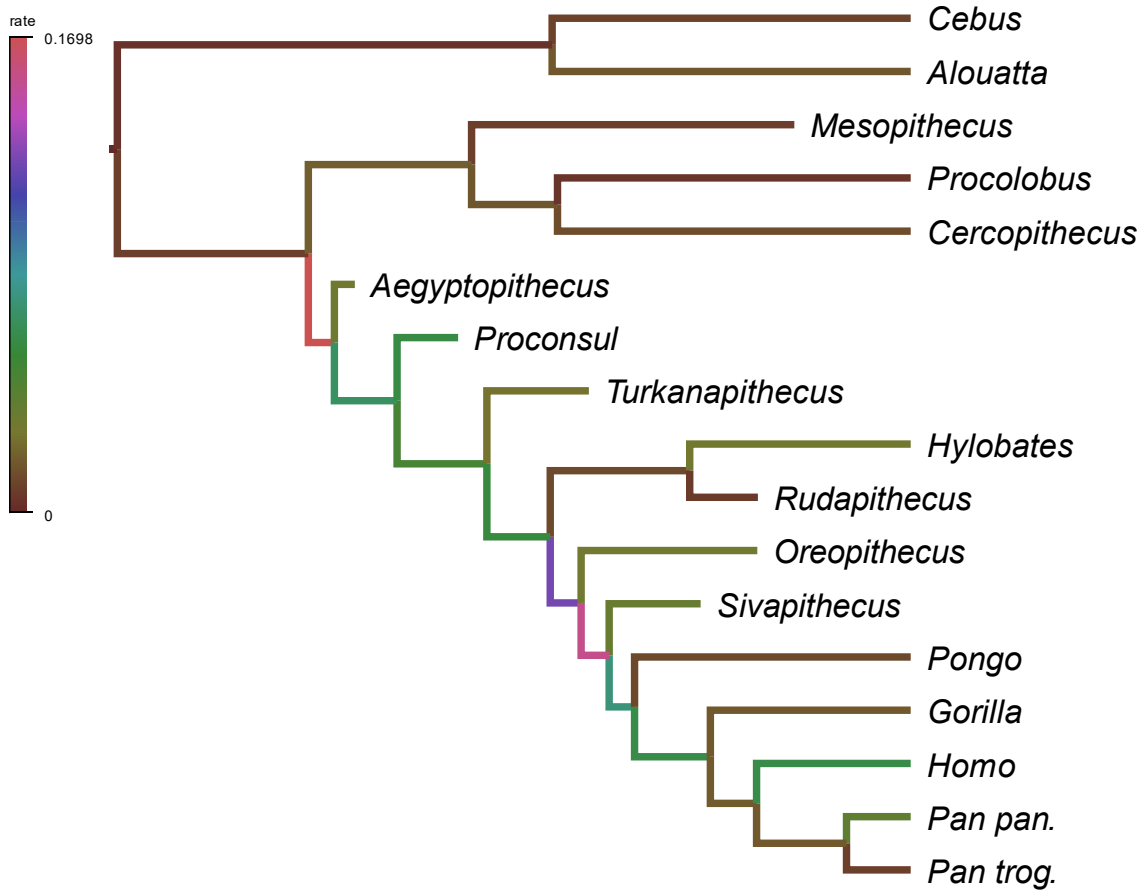


873

874 *Figure 4.* Placements of fossil genera on extant reference tree. Branch colors correspond

875 to evolutionary rate along individual branches.

876

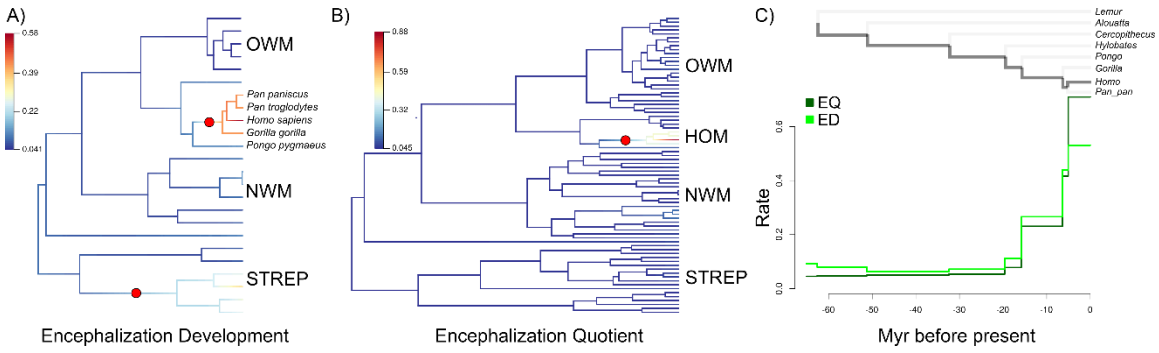


877

878 *Figure 5.* Rate shifts in A) encephalization development, and B) encephalization quotient.

879 C) Branch-specific evolutionary rates when tracing the lineage from *Homo* to the root.

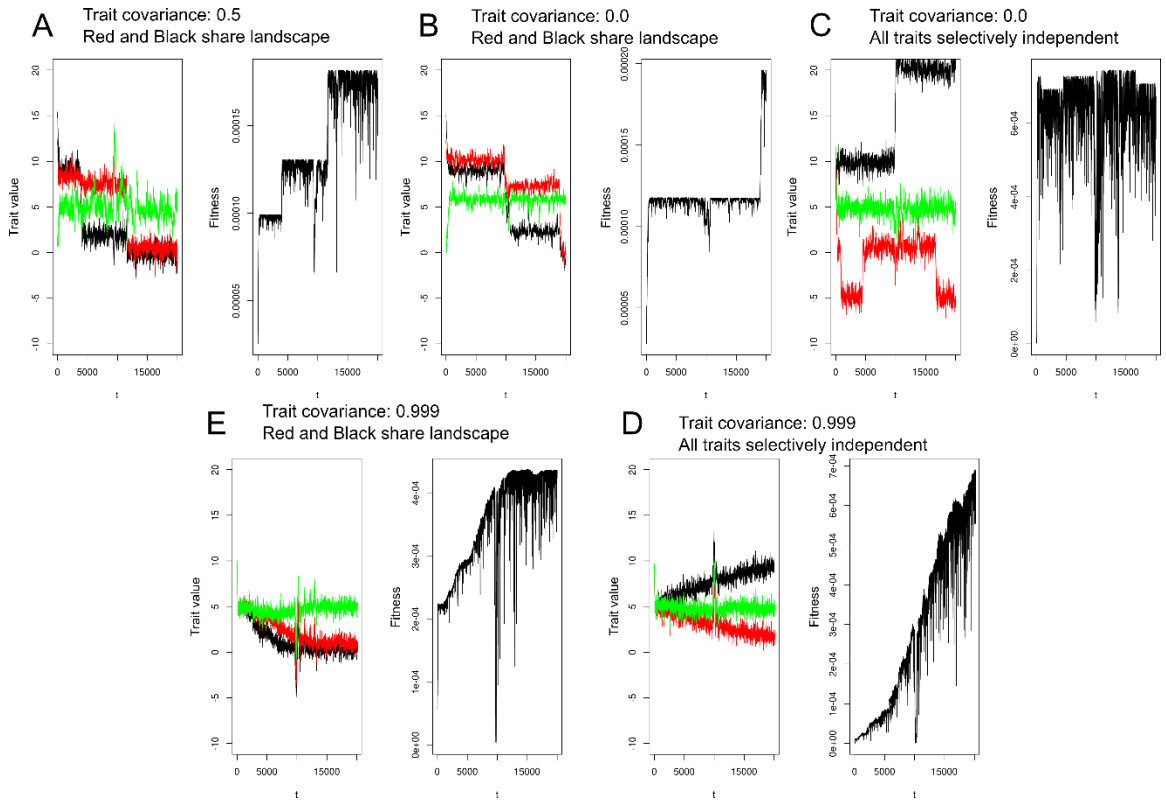


*Figure 6.* Monte Carlo simulations of integrated and atomized systems of three continuous traits. Each box is a simulated diffusion between three traits under A) moderate developmental linkage and shared selection, B) no developmental linkage and shared selection, C) no developmental linkage and selective independence, D) high developmental linkage and selective independence, and E) high developmental linkage and shared selection.

| suite | skeletal region | trait |
|---|---|---|
| 0 | Ulna | Olecranon length |
| 0 | Ulna | Middle shaft shape |
| 0 | Ulna | Olecranon shape |
| 0 | Ulna | Distal shape |
| 0 | Ulna | Styloid process length |
| 0 | Ulna | Proximal shaft shape |
| 0 | Ulna | Coronoid |
| 0 | Ulna | Trochlea notch shape |
| 0 | Humerus | Head P D shape |
| 0 | Humerus | Trochlea |
| 0 | Humerus | Intertubercular angle |
| 0 | Humerus | Lat. trochlea keel dev. |
| 0 | Humerus | Bicipital groove shape |
| 0 | Humerus | Humeral Head Size |
| 0 | Humerus | Head torsion |
| 0 | Humerus | Trochlea sup. notch angle |
| 0 | Humerus | Zona conoidea dist. depth |
| 0 | Humerus | Grt. tuberosity proj. |
| 0 | Carpus | Capitate head M L width |
| 0 | Carpus | Capitate M C 3 shape |
| 0 | Carpus | CAPCM4 |
| 0 | Carpus | Hamate DP depth COR |
| 0 | Carpus | Capitate head A P / P D |
| 0 | Carpus | Capitate dorsal nonarticular |
| 0 | Carpus | Capitate M C 3 depth |
| 0 | Carpus | Lunate dist. |

| | |
|---|---|
| 0 Carpus | Hamate triquetral facet angle |
| 0 Carpus | Capitate M C 2 facets |
| 0 Cranium | Grt. palatine foramen position |
| 0 Cranium | Zygomatic root origin elevation |
| 0 Cranium | Basicranial length |
| 0 Cranium | Piriform aperture shape |
| 0 Cranium | Postglenoid projection |
| 0 Cranium | Basicranium vs. palate |
| 0 Cranium | Bregma position |
| 0 Cranium | Lacrimal fossa & orbital floor |
| 0 Cranium | Facial projection |
| 0 Cranium | Zygomax. tubercle A P width |
| 0 Cranium | Basicranium vs. nuchal |
| 0 Cranium | Nasoalveolar clivus length |
| 0 Cranium | Head M L shape |
| 0 Cranium | Zygomatic |
| 0 Cranium | Face height vs. depth |
| 0 Cranium | Piriform max. M L elevation |
| 0 Cranium | Neurocranial shape |
| 0 Cranium | Asterion angle |
| 0 Radius | Lunate facet shape |
| 0 Radius | Lunate facet angle |
| 0 Radius | Neck shape |
| 0 Radius | Scapholunate facet areas |
| 0 Radius | Lunate facet dorsal proj. |
| 0 Radius | Distal facets area |
| 0 Radius | Total length |

| | |
|---|---|
| 0 Radius | Radial neck length |
| 0 Radius | Shaft curvature M L |
| 0 Radius | Head articular surface P D |
| 0 Scapula | Trapezius insert angle |
| 0 Scapula | Coraco |
| 0 Scapula | Inf. glenoid cor |
| 0 Scapula | Acromian size |
| 0 Scapula | Inferior angle |
| 0 Scapula | Sup. notch shape |
| 0 Scapula | Spinatus ratio |
| 0 Scapula | Glenoid vent. bar angle |
| 0 Pelvis | pubic symphysis length |
| 1 Ulna | Ulna head height |
| 1 Ulna | Semilunar keel angle |
| 1 Ulna | Radial notch shape |
| 1 Ulna | Distal shaft shape |
| 1 Humerus | Dist. articular shape |
| 1 Humerus | Trochlea dist. waisting |
| 1 Humerus | Med. trochlea keel dev. |
| 1 Humerus | Olecranon fossa depth |
| 1 Humerus | Olecranon fossa shape |
| 1 Carpus | Capitate P D length |
| 1 Carpus | Hamate M C 4 |
| 1 Carpus | Lunate radial facet M L |
| 1 Carpus | Lunate triquetral facet shape |
| 1 Cranium | Piriform base M L width |
| 1 Cranium | M1 shape |

| | |
|---|---|
| 1 Cranium | Lsr. palatine foramen |
| 1 Cranium | Molar crown areas |
| 1 Cranium | Entoglenoid width |
| 1 Cranium | Entoglenoid projection |
| 1 Cranium | Nasal bone M L width |
| 1 Cranium | Orbital margin M L width |
| 1 Cranium | Orbit area |
| 1 Cranium | Interorbital width |
| 1 Radius | Distal surface shape |
| 1 Radius | Styloid process length |
| 1 Radius | Radial Head Shape |
| 1 Manubrium | Manubrium shape |
| 1 Scapula | Scapula Body shape |
| 1 Scapula | Trapezius med. insert |
| 1 Scapula | Superior angle |
| 1 Scapula | Subscapular depth |
| 1 Scapula | Vertebral border length |
| 1 Scapula | Glenoid fossa shape |
| 1 Scapula | Coracoid length |
| 1 Pelvis | illium length |
| 1 Pelvis | bi |
| 1 Pelvis | anteroposterior pelvic diameter |
| 1 Pelvis | pelvic length |
| 2 Humerus | Epicondyles projection |
| 2 Humerus | Olecranon perforation |
| 2 Ulna | Shaft curvature A P |
| 2 Carpus | Capitate M C 3 waisting |

| | |
|---|---|
| 2 Carpus | Capitate waisting |
| 2 Carpus | Lunate PD Length |
| 2 Carpus | Hamate hamulus P D proj. |
| 2 Carpus | Capitate M C 2 margin |
| 2 Carpus | Capitate M C 2 orientation |
| 2 Carpus | Lunate dist. facet shape |
| 2 Cranium | Orbit shape |
| 2 Cranium | Pterion post. config |
| 2 Cranium | Palate shape |
| 2 Cranium | Lacrimal fossa visibility |
| 2 Cranium | Palatine width |
| 2 Cranium | Postorbital constriction |
| 2 Cranium | Palate depth |
| 2 Radius | Head depth P D |
| 2 Scapula | Glenoid fossa depth |
| 2 Pelvis | illium width |
| 2 Pelvis | ischium length |
| 2 Pelvis | AIIS to hip joint |
| 2 Pelvis | inferior pubic ramus length |
| 2 Pelvis | acetabulum diameter |
| 2 Pelvis | superior pubic ramus length |
| 3 Scapula | Spinoglenoid notch depth |
| 3 Scapula | Infraglenoid tuberosity M L |
| 3 Pelvis | lower illiac height |
| 3 Pelvis | inferior pubic ramus cross |
| 3 Ulna | Radial notch depth |
| 3 Cranium | Temporal fossa width |

| | |
|---|---|
| 3 Cranium | Face vs. nasal height |
| 3 Cranium | Face height vs. width |
| 3 Cranium | Palate width |
| 3 Cranium | Entoglenoid lat. pterygoid |
| 3 Humerus | Medial trochlea keel & medial epicon |
| 4 Pelvis | ischium cross |
| 4 Pelvis | superior pubic ramus cross |
| 4 Pelvis | upper illiac height |
| 4 Pelvis | lower ilium cross |
| 4 Pelvis | ischium dorsal projection |
| 4 Pelvis | pubic symphysis |
| 4 Pelvis | auricular surface area |
| 4 Pelvis | biacetabular diameter |
| 4 Pelvis | maximum transverse diameter |
| 4 Pelvis | sacrum width |

893

894 **Table S1:** List of traits and their skeletal regions that comprise each of the mosaic suites detected
895 from the skeletal data.

896